HHS Public Access

Author manuscript

*Cell Rep*. Author manuscript; available in PMC 2018 December 11.

Published in final edited form as:

*Cell Rep*. 2018 October 30; 25(5): 1204–1213.e4. doi:10.1016/j.celrep.2018.10.002.

# Differential Roles of IL-2 Signaling in Developing versus Mature Tregs

**Martin Y. Fan**[1,2], **Jun Siong Low**[3], **Naoki Tanimine**[1], **Kelsey K. Finn**[1,2], **Bhavana Priyadharshini**[1], **Sharon K. Germana**[1], **Susan M. Kaech**[3,4,5], and **Laurence A. Turka**[1,2,6,*]

[1]Department of Surgery and Center for Transplantation Sciences, Massachusetts General Hospital, Harvard Medical School, Boston, MA 02129, USA

[2]Program in Immunology, Division of Medical Sciences, Harvard Medical School, Boston, MA 02115, USA

[3]Department of Immunobiology, Yale University School of Medicine, New Haven, CT 06520, USA

[4]The Salk Institute for Biological Studies, La Jolla, CA 92037, USA

[5]Howard Hughes Medical Institute, Chevy Chase, MD 20815, USA

[6]Lead Contact

## SUMMARY

Although Foxp3$^{+}$ regulatory T cells (Tregs) require interleukin-2 (IL-2) for their development, it has been unclear whether continuing IL-2 signals are needed to maintain lineage stability, survival, and suppressor function in mature Tregs. We generated mice in which CD25, the main ligand-binding subunit of the IL-2 receptor, can be inducibly deleted from Tregs after thymic development. In contrast to Treg development, we find that IL-2 is dispensable for maintaining lineage stability in mature Tregs. Although continuous IL-2 signaling is needed for long-term Treg survival, CD25-deleted Tregs may persist for several weeks *in vivo* using IL-7. We also observe defects in glycolytic metabolism and suppressor function following CD25 deletion. Thus, unlike developing Tregs in which the primary role of IL-2 is to initiate Foxp3 expression, mature Tregs require continuous IL-2 signaling to maintain survival and suppressor function, but not to maintain lineage stability.

## Graphical Abstract

*Correspondence: lturka@partners.org.

AUTHOR CONTRIBUTIONS

M.Y.F. and L.A.T. designed the study and wrote the manuscript. J.S.L. and S. M.K. helped design adoptive transfer experiments involving cytokine-deficient mice, which were performed by M.Y.F. and J.S.L.; N.T. and B.P. helped design the Seahorse metabolic flux experiments, which were performed by M.Y.F. and N.T.; M.Y.F. and K.K.F. designed and performed the EAE experiments; and S.K.G. helped design long range PCR (LRPCR) primers.

SUPPLEMENTAL INFORMATION

Supplemental Information includes six figures and one table and can be found with this article online at https://doi.org/10.1016/j.celrep.2018.10.002.

DECLARATION OF INTERESTS

The authors declare no competing interests.

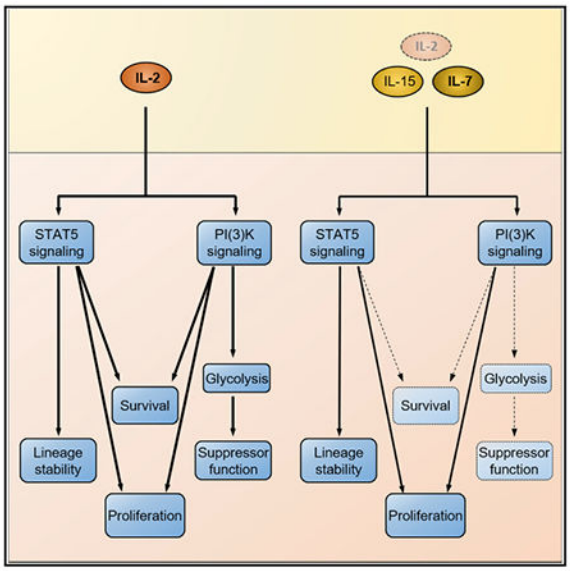


## In Brief

Interleukin-2 (IL-2) is important for regulatory T cell (Treg) development and is believed to be necessary for Treg survival and lineage stability. Here, Fan et al. show that IL-2 is in fact dispensable for Treg lineage maintenance *in vivo* and that Tregs may persist for an extended time *in vivo* using IL-7.

## INTRODUCTION

$CD4^+$ $Foxp3^+$ regulatory T cells (Tregs) are critical for immune homeostasis (Sakaguchi et al., 1995; Hori et al., 2003). Most Tregs express high levels of CD25, the alpha subunit of the interleukin-2 (IL-2) receptor (IL-2R), and Tregs are the only cell type known to constitutively express the full receptor trimer (Malek, 2008). While it is generally assumed that continued IL-2 signaling is needed for Treg survival, suppressor function, and lineage maintenance, these inferences have largely been extrapolated from germline knockout models, blocking antibody experiments, and *in vitro* studies. The roles of continued IL-2 signaling following Treg development, and the signals by which IL-2 executes these roles, remain imperfectly understood (Chinen et al., 2016).

The IL-2R trimer is composed of CD25, CD122, and CD132 (Stauber et al., 2006). CD122 and CD132 are capable of low-affinity IL-2 binding and activate the signal transducer and activator of transcription (STAT)5, phosphatidylinositol 3-kinase (PI(3)K), and mitogen-activated protein kinase (MAPK)/extracellular signal-regulated kinase (ERK) pathways. CD25 does not contain a signaling domain but rather confers a roughly 1,000-fold higher ligand affinity to the receptor trimer. IL-2 is important for Treg development, as demonstrated by defects in mice deficient for either CD25 or IL-2. In the absence of IL-2, Treg precursors appear to rely primarily on IL-15 for induction of Foxp3 (Lio and Hsieh, 2008). Among the signals delivered via the IL-2R, STAT5 is critical for Treg development,

as initial Foxp3 expression requires binding of gene regulatory elements by STAT5, and $STAT5^{-/-}$ mice are essentially devoid of Tregs (Zorn et al., 2006; Burchill et al., 2007).

Although knockout mice lacking IL-2 signaling elements display a common set of autoimmune phenotypes (Willerford et al., 1995; Fontenot et al., 2005), it has been difficult to address whether this is due to defects in Treg development or in Treg function. These models are also insufficient to address how IL-2 affects the survival, function, and lineage stability of mature Tregs, since the development of lethal autoimmunity in these mice confounds comparisons with wild-type Tregs under resting immune conditions. Additionally, because IL-2 plays an important role in Treg development (Lio and Hsieh, 2008), it remains possible that Tregs that mature in IL-2 or CD25 knockout mice develop an altered T cell receptor (TCR) repertoire that does not provide for optimal maintenance of self-tolerance.

Attempts to address the role of IL-2 in mature Tregs with blocking antibodies are inconclusive. While the anti-CD25 monoclonal antibody PC61 leads to a rapid loss of Tregs, this is now recognized to occur through phagocytic clearance rather than IL-2 deprivation (Onizuka et al., 1999; Setiady et al., 2010). True blocking antibodies such as 7D4 (anti-CD25) and S4B6 (anti-IL-2) in fact yield mixed results with regards to Treg survival (Kohm et al., 2006; Couper et al., 2007; Rubtsov et al., 2010; Setoguchi et al., 2005). Therefore, a number of open questions remain concerning the roles of IL-2 in Treg survival, lineage stability, and suppressor function, particularly under homeostatic immune conditions. It is also unclear whether particular Treg subsets may tolerate IL-2 deprivation and what alternative cytokines mature Tregs might rely on *in vivo.*

To address these issues, we developed an inducible genetic system to delete CD25 in mature, post-thymic Tregs. Using this system, we demonstrate that IL-2 is necessary to maintain long-term Treg survival, but not Foxp3 expression, under resting immune conditions. Although the surface phenotypes of CD25-deleted Tregs resembled those of circulating wild-type $CD25^{lo}$ Tregs, we found the majority of CD25-deleted Tregs actually derived from $CD25^{hi}$ precursors. In the absence of IL-2, this population relied on IL-7 to prolong its survival. CD25-deleted Tregs also showed defects in their glycolytic metabolism and ability to suppress immune activation *in vitro.* Thus, in contrast to developing Tregs, in which the primary role of IL-2 is to initiate Foxp3 expression via a STAT5-dependent mechanism, IL-2 in mature Tregs is needed to maintain survival and suppressor function but is dispensable for lineage stability. Compensation for IL-2 loss with IL-7, rather than IL-15, also suggests a differential usage of signaling pathways downstream of the common gamma chain in developing versus mature Tregs.

## RESULTS

### Generation and Validation of $CD25^{fl/fl}$ × Rosa-RFP × $Foxp3^{EGFP\text{-}Cre\text{-}ERT2}$ "CD25-iΔTreg" mice

The gene for CD25 *(Il2ra)* consists of 8 exons encoding 2 extra-cellular domains and 1 transmembrane domain (Malek, 2008). We generated chimeric mice using embryonic stem cells in which exon 4 (encoding one of two extracellular domains) is flanked by *loxP* sites

(Figure S1A). Loss of this exon is known to abolish binding to IL-2 (Leonard et al., 1984). Resultant "$CD25^{fl/fl}$" mice were bred with $Foxp3^{YFP\text{-}Cre}$ mice (Rubtsov et al., 2008) to confirm that exon 4 deletion yielded functional effects consistent with known knockout phenotypes. By 2.5 weeks after birth, $CD25^{fl/fl}$ × $Foxp3^{YFP\text{-}Cre}$ mice developed enlarged lymph nodes and thymic involution (Figure S2A) with a reduced percentage of splenic $Foxp3^+$ cells (Figure S2B) and increased percentages of activated $CD4^+$ $CD44^+$ $CD69^+$ conventional T cells (Tconv) (Figure S2C). No $CD25^{fl/fl}$ × $Foxp3^{YFP\text{-}Cre}$ mice survived beyond 3.5 weeks. Nearly identical phenotypes have been described in mice lacking CD25 or IL-2 entirely (Willerford et al., 1995; Sadlack et al., 1993) and in a recent study in which an independently derived $CD25^{fl/fl}$ line was crossed with $Foxp3^{YFP\text{-}Cre}$ (Chinen et al., 2016), confirming that deletion in the $CD25^{fl}$ allele recapitulates functional loss of CD25.

To study the role of IL-2 in post-developmental Tregs, we obtained mice bearing a tamoxifen-inducible $Foxp3^{EGFP\text{-}Cre\text{-}ERT2}$ construct (Rubtsov et al., 2010), which causes $Foxp3^+$ cells to express EGFP and a Cre recombinase that only enters the nucleus after tamoxifen exposure. We also obtained a Rosa-RFP recombination reporter line (Luche et al., 2007) to label $Foxp3^+$ cells present at the time of tamoxifen exposure and track potential loss of Foxp3 expression. Thus, two strains of mice were generated: (1) a $CD25^{fl/fl}$ × Rosa-RFP × $Foxp3^{EGFP\text{-}Cre\text{-}ERT2}$ strain featuring CD25-inducible deletion among Tregs, which we refer to as CD25-iΔTreg mice; and (2) a $CD25^{+/+}$ × Rosa-RFP × $Foxp3^{EGFP\text{-}Cre\text{-}ERT2}$ control strain, which we refer to as WT mice.

By 4 days after the first tamoxifen injection, the majority of all $Foxp3^+$ cells from CD25-iΔTreg mice lose CD25 (Figure S3A), with surface expression comparable to that of unstimulated $Foxp3^-$ $CD4^+$ Tconv (Figures S3B and S3C). Deletion was restricted to Cre-expressing cells, as $Foxp3^-$ $CD4^+$ and $CD8^+$ T cells from CD25-iΔTreg mice expressed CD25 upon stimulation (Figure S3D). The Rosa-RFP reporter was rapidly activated, with a distinct $RFP^+$ population appearing 4 days after the first tamoxifen injection (Figure S3E). 90% of $RFP^+$ $Foxp3^+$ cells in CD25-iΔTreg mice had deleted CD25 (Figure S3G), and we refer to these $CD25^-$ $RFP^+$ $Foxp3^+$ cells as CD25-iΔTregs (Figure S3F). We also refer to the $RFP^+$ $Foxp3^+$ population in wild-type (WT) mice as WT-Tregs and further stratify these cells into WT $CD25^{hi}$ and WT $CD25^{lo}$ subsets. Deletion of CD25 was not always reflected by activation of the RFP reporter, as many $CD25^-$ Tregs failed to express RFP (Figure S3H). However, because thymic output continues beyond the course of tamoxifen treatment, the $RFP^-$ population contains an indeterminate mixture of CD25 expressing and CD25-deleted Tregs. We therefore refer to the collective $RFP^-$ population as "$RFP^-$ $CD25^{fl/fl}$" or "$RFP^-$ $CD25^{+/+}$" Tregs.

## Loss of Tregs and Maintenance of Foxp3 following CD25 Deletion

To assess how CD25 loss impacts Treg homeostasis, mice were given intraperitoneal tamoxifen to induce CD25 deletion (Figure 1A), and blood samples were obtained over a period of 10 weeks. We found that following tamoxifen injection, CD25-iΔTregs were lost with a half-life of ~2 weeks (Figure 1B). As with the above characterization studies, 90% of $RFP^+$ $Foxp3^+$ cells lost CD25 immediately after tamoxifen administration; the remaining 10% steadily comprise a greater percentage of the $RFP^+$ $Foxp3^+$ population over time, likely

due to a survival advantage over $RFP^+$ CD25-deleted Tregs (Figure 1C). No differences were observed between male and female mice (data not shown). In both WT and CD25-iΔTreg mice, the total percentage of $Foxp3^+$, $CD4^+$, and $CD8^+$ T cells remained the same (Figures 1D, S4A, and S4B). Total Treg numbers were maintained in CD25-iΔTreg mice by new thymic output as demonstrated by increased expression of CD31, a marker of recent thymic emigrants, among $RFP^-$ $CD25^{fl/fl}$ Tregs (Figure 1E). These newly generated cells have not been exposed to tamoxifen, are mostly $CD25^{hi}$, and rapidly comprise the majority of the $RFP^-$ $CD25^{fl/fl}$ Treg population (Figure S4C).

While no differences were observed in BrdU uptake between CD25-iΔTregs, WT $CD25^{lo}$ Tregs, and WT $CD25^{hi}$ Tregs (Figure 1F), we found an increase in the percentage of apoptotic CD25-iΔTregs as measured by Annexin-V × 7-AAD staining (Figure 1G). $RFP^-$ $CD25^{fl/fl}$ Tregs, in contrast, showed increases in bromodeoxyuridine (BrdU) uptake, but not in cell death (Figures S4D and S5E). This likely reflects increased proliferation to compensate for the death of CD25-iΔTregs to maintain total Treg percentages in CD25-iΔTreg mice. Preferential sequestration could not account for the loss of CD25-iΔTregs from the blood, as all major lymphoid organs showed similar losses of CD25-iΔTregs 2 weeks following tamoxifen injection (Figures S4F-S4J). No $RFP^+$ cells were observed in any organs prior to tamoxifen administration, confirming no “leakiness” of the Rosa-RFP reporter. These results implicate cell death as the primary cause for the loss of Tregs following CD25 depletion.

$Foxp3^-$ $CD4^+$ and $CD8^+$ T cells constitute the primary sources of IL-2 *in vivo* (Malek, 2008; Liu et al., 2015) and are more sparsely distributed in peripheral tissues than in lymphoid organs. Since Tregs in these environments might have adapted to reduced IL-2 availability, we examined whether they were less susceptible to death following CD25 deletion. We selected the liver as one such peripheral tissue site and used another, visceral adipose tissue (VAT), for comparison due to ready availability of IL-2 from VAT-resident invariant natural killer T cell (iNKT) cells (Lynch et al., 2015). In both tissues, we observed losses of Tregs to a similar magnitude as seen in lymphoid organs following CD25 deletion (Figures S4K and S4L).

In prior studies, blocking antibodies against IL-2 or CD25 has led to reductions in Foxp3 expression among Tregs, suggesting that continuous IL-2 signaling in post-thymic Tregs is necessary to maintain Foxp3 expression (Kohm et al., 2006; Rubtsov et al., 2010). Since antibodies only temporarily block IL-2 signaling, it has not been certain whether continued IL-2 signaling is needed to maintain long-term Treg lineage stability. We found that although Foxp3 levels were reduced shortly following CD25 deletion, Foxp3 expression was maintained without further losses for the next 10 weeks (Figure 2A). Gating on $RFP^+$ Tregs revealed a unimodal Foxp3 histogram in both genotypes, with no evidence for a distinct $RFP^+$ $FoxP3^-$ “ex-Treg” population as far as 10 weeks after tamoxifen injection (Figure 2B). Interestingly, although average FoxP3 expression among CD25-iΔTregs was ~20% lower than that of WT $CD25^{hi}$ Tregs, it was similar to that of WT $CD25^{lo}$ Tregs (Figures 2A and 2C).

## Phenotypic Resemblance of CD25-iΔTregs to WT CD25$^{lo}$ Tregs

Numerous subsets of Tregs have been described in recent years, including peripherally induced Tregs (pTregs), which derive from CD4$^{+}$ CD25$^{−}$ naive T cells, express lower levels of CD25 than thymically derived Tregs (tTregs), and may develop in the absence of IL-2 (D'Cruz and Klein, 2005). While it was possible pTregs might be less dependent than tTregs on IL-2 and possess a survival advantage following CD25 deletion (Malek, 2008), we did not observe any differences in Helios or Neuropilin-1 expression among CD25-iΔTregs, WT CD25$^{lo}$ Tregs, and WT CD25$^{hi}$ Tregs, suggesting no enrichment of pTregs among the CD25-iΔTreg population (Figures S5A and S5B). Tregs may also be divided into central (cTreg) and effector (eTreg) subsets, with the latter enriched among CD25$^{lo}$ Tregs (Fisson et al., 2003; Smigiel et al., 2014). Consistent with published results, we found an increase in CD44$^{hi}$ CD62L$^{lo}$ cells among both WT CD25$^{lo}$ and CD25-iΔTregs as compared to WT CD25$^{hi}$ Tregs (Figure S5C). A greater percentage of CD25-iΔTregs expressed PD-1 and ICOS compared to WT CD25$^{hi}$ Tregs (Figures 3A and 3B), while the expression of other major Treg surface molecules such as GITR and CTLA-4 was only slightly reduced in CD25-iΔTregs (Figures S5D-S5F). Similar observations were made when comparing WT CD25$^{lo}$ to WT CD25$^{hi}$ Tregs. For most surface molecules, CD25-iΔTregs strongly resembled WT CD25$^{lo}$ Tregs (Figures 3 and S5).

## Origins of Surviving CD25-iΔTregs

Because of the phenotypic similarity between CD25-iΔTregs and WT CD25$^{lo}$ Tregs, we asked whether the surviving CD25-iΔTregs derived primarily from CD25$^{hi}$ Tregs that had lost CD25 and adopted CD25$^{lo}$ characteristics or whether they derived from preferential survival of the CD25$^{lo}$ population. To test whether CD25$^{hi}$ or CD25$^{lo}$ Tregs could contribute to the CD25-iΔTreg population, we tracked the fate of each subset in an adoptive transfer model. CD25$^{hi}$ and CD25$^{lo}$ Foxp3$^{+}$ cells were sorted from WT and CD25-iΔTreg mice not exposed to tamoxifen and then transferred in equal numbers into separate CD45.1$^{+}$ congenic recipients. Mice received tamoxifen after 1 week (Fisson et al., 2003) and were euthanized 2 weeks later. All CD4$^{+}$ splenocytes were collected to measure total splenic recovery of transferred CD45.2$^{+}$ cells (Figures 4A and 4B). Nearly all cells from CD25-iΔTreg donors lost CD25 (Figures 4C and 4D). By gating out host CD45.1$^{+}$ cells, we were able to exclude new thymic output from the CD45.2$^{+}$ RFP$^{−}$ population. We noted an equal ratio of RFP$^{+}$ to RFP$^{−}$ Tregs among cells from both CD25-iΔTreg and WT donors (Figure 4E), indicating that the expression of RFP had no effect on cell survival. Importantly, we observed that both Tregs that were initially CD25$^{hi}$ and those that were initially CD25$^{lo}$ could survive after CD25 deletion, indicating that both groups can contribute to the CD25-iΔTreg population (Figure 4F). However, because CD25$^{hi}$ precursors showed increased survival following CD25 deletion, and because CD25$^{hi}$ cells comprise the majority of all Tregs prior to tamoxifen treatment, we conclude that the majorityof CD25-iΔTregs derive from CD25 precursors based upon a survival advantage.

## Reduced Suppressor Function and Glycolysis among CD25-iΔTregs

To test whether Treg suppressor function was affected by loss of IL-2 signaling, we used a rapid *in vitro* suppression assay in which the primary readout was expression of the

activation markers CD69 and CD154 (CD40L) among target cells 7 hr after activation in co-culture (Canavan et al., 2012; Ruitenberg et al., 2011). We found that CD25-iΔTregs were less effective than WT Tregs at suppressing target cell upregulation of CD69 and CD154 (Figures 5A and 5B).

We further evaluated Treg function *in vivo* using an experimental autoimmune encephalomyelitis (EAE) model in which disease induction is Treg independent but disease stabilization and remission requires functional Tregs (Kohm et al., 2002). Mice were given tamoxifen both prior to EAE induction and again after 2 weeks to ensure a majority of Tregs lacked CD25 throughout the course of the experiment. Although no differences were observed in the onset or initial severity of EAE, CD25-iΔTreg mice failed to undergo the Treg-dependent disease remission phase (Figure 5C). These results indicate diminished *in vivo* suppressor function among Tregs in the absence of continuous IL-2 signaling.

Glycolytic metabolism is needed for full Treg suppressor function *in vivo*, as it promotes expression of key Treg effector molecules such as CTLA-4 and promotes Treg proliferation (Newton et al., 2016; Zeng et al., 2013; Gerriets et al., 2016). We therefore investigated the effects of IL-2 signaling loss on Treg metabolism using a Seahorse flux analyzer to measure extracellular acidification rate (ECAR), a marker of glycolytic flux. As shown in Figures 5D–5F, IL-2 enhances glycolysis in all Tregs (i.e., WT $CD25^{hi}$ Tregs, WT $CD25^{lo}$ Tregs, and CD25-iΔTregs), with by far the greatest increase being seen in the WT $CD25^{hi}$ Treg subset. This is consistent with levels of high-affinity IL-2R expression, and we attribute the effects of IL-2 in WT $CD25^{lo}$ Tregs and CD25-iΔTregs to effects mediated via the lower-affinity beta and gamma subunits of the IL-2 receptor. IL-7 did not increase glycolysis in WT $CD25^{hi}$ Tregs but had small effects (i.e., similar to those seen with IL-2) in WT $CD25^{lo}$ Tregs and CD25-iΔTregs. The same cytokine treatments had negligible effects on the glycolysis of Tconv (data not shown).

## IL-7 Is Less Effective than IL-2 at Maintaining Downstream Signals

STAT5 signaling is known to promote Treg survival and suppressor function (Chinen et al., 2016). While IL-2 constitutes the primary source of STAT5 signals in Tregs, other common gamma chain cytokines such as IL-7 and IL-15 may also fill this role. We found that among unstimulated cells, a greater percentage of CD25-iΔTregs phosphorylated STAT5 in response to IL-7 than either WT $CD25^{hi}$ or WT $CD25^{lo}$ Tregs, while no differences were observed in STAT5 responses to IL-15 (Figure S6A). This was consistent with surface expression data for the relevant cytokine receptors. CD127, the alpha subunit of the IL-7 receptor, was elevated in CD25-iΔTregs relative to WT-Tregs (Figure 3C), suggesting that CD25-iΔTregs might rely on IL-7 following CD25 deletion. CD25-iΔTregs showed no increases compared with WT-Tregs in CD122 or CD132, the beta and gamma subunits shared between the IL-2 and IL-15 receptors (Figures S5G and S5H), and failed to express CD215, the alpha subunit of the IL-15 receptor (Figure S5I).

Since processes such as cellular metabolism are dependent on PI(3)K rather than STAT5 signaling, we also examined how reliance on IL-7 or IL-15 might affect signaling along all IL-2 downstream pathways. WT $CD25^{hi}$ $Foxp3^{+}$ Tregs were stimulated overnight with plate-bound anti-CD3/CD28 and analyzed for activation of the STAT5, PI(3)K, and ERK

pathways. As expected, nearly all cells had activated the STAT5, PI(3)K, and ERK signaling pathways after stimulation. We then transferred the cells to new wells lacking any TCR stimulus and incubated them for 24 hr with IL-2, IL-15, IL-7, or no cytokine. We found that IL-2 was more effective than either IL-7 or IL-15 in maintaining signaling along all downstream pathways, including PI(3)K signaling (Figures 6A–6C). Although neither cytokine could maintain downstream signals as well as IL-2, both were still effective compared to the no cytokine condition.

### CD25-iΔTregs Rely on IL-7 for Survival

Finally, to evaluate the roles of IL-15 and IL-7 in the homeostasis of CD25-iΔTregs, we used an adoptive transfer approach to deprive CD25-iΔTregs of either cytokine. After administering tamoxifen and sorting CD25-iΔTregs or WT $CD25^{hi}$ Tregs, we transferred the cells into WT, IL-15 knockout (KO), or IL-7 KO hosts with an equal number of $CD45.1^{+}$ $CD25^{hi}$ cells as a reference population. Recipient mice were sacrificed after 2 weeks, and recovery of $RFP^{+}$ cells was measured (Figures 6D-6F). No survival differences were observed among WT-Tregs, indicating that IL-7 and IL-15 are dispensable for Treg survival in the presence of IL-2 (Figure 6G). Because of the similarity between the IL-2 and IL-15 receptors and their downstream gene expression profiles (Ring et al., 2012), we expected that IL-15 would be the primary cytokine compensating for IL-2. However, we found only a modest and nonstatistically significant decrease in the survival of CD25-iΔTregs transferred into IL-15 KO hosts. A larger and statistically significant exacerbation of cell death was instead observed among CD25-iΔTregs transferred to IL-7 KO hosts (Figure 6H). Foxp3 expression was not significantly affected following transfer into either KOt host (Figures S6B-S6D).

## DISCUSSION

In prior KO models, the roles of continued IL-2 signaling in Tregs have been confounded by systemic autoimmunity and the possibility of altered Treg development. Using inducible genetic deletion of CD25, we have performed studies specifically examining the roles of IL-2 in post-thymic Tregs under resting immune conditions. In contrast with developing Tregs, for which a primary role of IL-2 is to initiate Foxp3 expression (Burchill et al., 2007), we found that IL-2 is dispensable for Foxp3 maintenance in mature Tregs. Foxp3 levels were reduced in the absence of IL-2 signaling, but cells did not become Foxp3-negative “ex-Tregs.” We also found that further deprivation of IL-15 or IL-7 in CD25-deleted Tregs did not affect Foxp3 levels. This again contrasted with Treg development, where IL-2/IL-15 double-KO mice are known to generate fewer $Foxp3^{+}$ cells than mice lacking IL-2 alone (Burchill et al., 2007).

During Treg development, at least one interleukin among IL-2, IL-15, or IL-7 must be present to generate $Foxp3^{+}$ cells, even if in limited numbers (Vang et al., 2008; Fan and Turka, 2018). While IL-2 is sufficient to induce Foxp3 expression among developing Tregs, in its absence, IL-15 is a more potent initiator of Foxp3 expression than IL-7 (Lio and Hsieh, 2008). On the other hand, we found that CD25-deleted mature Tregs could persist for several weeks using IL-7, while IL-15 had minimal effects on cell survival. The differential

preference for IL-7 and IL-15 in developing versus mature Tregs may be partially attributed to the localization of IL-2. In the thymus, IL-2 and IL-15 are both produced in the medulla (Malek, 2008; Cui et al., 2014), where Treg maturation occurs; although IL-7 may also be found in the medulla, the majority of IL-7 is produced in the cortex. In lymph nodes, IL-2 and IL-7 production overlap at the outer T cell zone paracortex, where Tregs undergo active STAT5 signaling, but neither is abundant within T cell zones where IL-15 is produced (Hara et al., 2012; Liu et al., 2015).

The differential reliance on IL-7 and IL-15 may also indicate a differing usage of downstream common gamma chain pathways in developing versus mature Tregs. While IL-15 and IL-2 activate similar downstream pathways (Ring et al., 2012), IL-7 is additionally known to promote glycerol import and increased longevity among memory $CD8^+$ T cells (Cui et al., 2015). We found that IL-15 and IL-7 are less potent than IL-2 at maintaining signaling through all its major downstream pathways including PI(3)K signaling, consistent with a previous report showing similar effects in $CD8^+$ T cells (Cornish et al., 2006). PI(3)K signaling is notable among downstream IL-2 pathways as an inducer of glycolytic metabolism, which is required for Tregs to achieve full suppressor function (Newton et al., 2016; Gerriets et al., 2016). In particular, mTORC1 activity promotes CTLA-4 expression through a cholesterol-metabolism-dependent mechanism (Zeng et al., 2013). We found that following CD25 deletion, Tregs exhibited reduced glycolytic capacity, expressed lower levels of CTLA-4, and displayed reduced suppressor function. This finding is particularly intriguing, since it has not been clear how IL-2 signaling may promote the expression of key Treg suppression molecules such as CTLA-4. Published microarray analyses have found similar gene expression profiles among WT $CD25^{hi}$ Tregs, WT $CD25^{lo}$ Tregs, and Tregs from IL-2 KO mice (Fontenot et al., 2005; Vahl et al., 2014), suggesting that the effects of IL-2 on Treg suppressor function occur post-transcriptionally. Consistent with this, our lab has shown that changes in PI(3)K signaling have minimal effects on Treg transcriptional signatures (Huynh et al., 2015). Thus, control of Treg suppressor function through glycolytic metabolism may offer a post-transcriptional link between IL-2 signaling and Treg suppressor function.

Approximately 10%−20% of circulating Tregs are $CD25^{lo}$ and may withstand CD25 deletion better than $CD25^{hi}$ Tregs. In an adoptive transfer model, we found that the baseline survival of $CD25^{lo}$ Tregs was lower than that of $CD25^{hi}$ Tregs. While CD25 deletion reduced the survival of $CD25^{hi}$ Tregs, these cells still maintained higher survival rates than $CD25^{lo}$ Tregs. Thus, although $CD25^{lo}$ Tregs might be considered less dependent on IL-2 for survival than $CD25^{hi}$ Tregs, their baseline survival appears to be limited due to cell-intrinsic differences other than lower IL-2 binding. Furthermore, a greater survival rate among $CD25^{hi}$ Tregs, even with losses resulting from CD25 deletion, indicated that the majority of CD25-deleted Tregs were previously $CD25^{hi}$. Given the strong resemblance between CD25-deleted Tregs and $CD25^{lo}$ Tregs in the expression of most Treg surface molecules, it is likely that major Treg surface phenotypes are enforced by continuous IL-2 signaling.

Our findings may inform a number of clinically relevant scenarios under which Tregs lose CD25. Aging leads to a decline in CD25 expression among Tregs, likely due to reduced IL-2 production, and may be tied to the late onset of autoimmune disorders such as rheumatoid

arthritis and multiple sclerosis (Nishioka et al., 2006; Raynor et al., 2013; Jagger et al., 2014). Furthermore, the anti-CD25 monoclonal antibodies daclizumab and ba-siliximab are US Food and Drug Administration (FDA) approved for the treatment of multiple sclerosis and renal allograft rejection, respectively (Reichert et al., 2005). Although their primary mechanism of action targets effector T cells through an NK cell-dependent mechanism, they also target Tregs (Bielekova et al., 2006; Rech et al., 2012) and might be predicted to exacerbate rather than resolve autoimmunity, given findings of prior studies in mice or humans lacking CD25 from birth (Willerford et al., 1995; Sharfe et al., 1997). Our discovery of prolonged survival in mature Tregs following CD25 deletion may resolve this apparent paradox. Moreover, the differential usage of downstream signaling pathways in developing versus mature Tregs raises the possibility of administering additional IL-7 or targeting signaling nodes other than STAT5, such as those affecting Treg glycolytic metabolism, to mitigate the negative effects of CD25 blockade or loss on Treg suppressor function.

## STAR★METHODS

### KEY RESOURCES TABLE

| REAGENT or RESOURCE | SOURCE | IDENTIFIER |
|---|---|---|
| Antibodies | | |
| anti-CD25, clone PC61 | BioLegend | Cat# 102033; RRID:A3_10895908 |
| anti-CD4, clone GK1.5 | BioLegend | Cat# 100434; RRID:A3_893324 |
| anti-CD8, clone 53-6.7 | BioLegend | Cat# 100734; RRID:A3_2075238 |
| anti-CD45.2, clone 104 | BioLegend | Cat# 109824; RRID:A3_830789 |
| anti-CD45.1, clone A20 | BioLegend | Cat# 110716; RRID:A3_313505 |
| anti-CD62L, clone MEL-14 | BioLegend | Cat# 104411; RRID:A3_313098 |
| anti-CD44, clone IM7 | BioLegend | Cat# 103023; RRID:A3_493686 |
| anti-CD69, clone H1.2F3 | BioLegend | Cat# 104527; RRID:A3_10900250 |
| anti-CD31, clone 390 | BioLegend | Cat# 102415; RRID:A3_493411 |
| anti-CD127, clone A7R34 | BioLegend | Cat# 135023; RRID:A3_10897948 |
| anti-CD122, clone TM-β1 | BioLegend | Cat# 123209; RRID:A3_940615 |
| anti-CD132, clone TUGm2 | BioLegend | Cat# 132307; RRID:A3_10643575 |
| anti-PD-1, clone RMP1-30 | BioLegend | Cat# 109109; RRID:A3_572016 |
| anti-ICOS, clone 7E.17G9 | BioLegend | Cat# 117406; RRID:A3_2122712 |
| anti-GITR, clone DTA-1 | BioLegend | Cat# 126311; RRID:A3_1134212 |
| anti-CTLA-4, clone UC10-4B9 | BioLegend | Cat# 106309; RRID:A3_2230158 |
| anti-Nrp-1, clone 3E12 | BioLegend | Cat# 145206; RRID:A3_2562032 |
| anti-CD25, clone 7D4 | eBioscience | Cat# 13-0252-82; RRID:A3_891428 |
| anti-CD215, clone DNT15Ra | eBioscience | Cat# 17-7149-82; RRID:A3_10718543 |
| anti-Helios, clone 22F6 | BioLegend | Cat# 137220; RRID:A3_10690535 |
| anti-Foxp3, clone FJK-16 s | eBioscience | Cat# 53-5773-82; RRID:A3_763537 |
| anti-p-STAT5, clone SRBCZX | eBioscience | Cat# 17-9010-41; RRID:A3_2573271 |
| anti-p-S6, clone cupk43k | eBioscience | Cat# 17-9007-42; RRID:A3_2573270 |
| anti-p-Akt, Ser473, clone SDRNR | eBioscience | Cat# 48-9715-41; RRID:A3_2574124 |
| anti-p-ERK1/2, clone MILAN8R | eBioscience | Cat# 17-9109-41; RRID:A3_2573293 |
| anti-p-Akt, Thr308, polyclonal | Cell Signaling Technology | Cat# 9275S; RRID:A3_329828 |
| anti-PTEN, clone A2B1 | BD Biosciences | Cat# 560003; RRID:A3_1645437 |
| anti-CD154, clone MR1 | BioLegend | Cat# 106510; RRID:A3_2561561 |
| LEAF purified anti-CD3, clone 2C11 | BioLegend | Cat# 100314; RRID:A3_312679 |
| LEAF purified anti-CD28, clone 37.51 | BioLegend | Cat# 102112; RRID:A3_312877 |
| Dynabeads Mouse T-Activator CD3/CD28 | Thermo Scientific | Cat# 11456D |
| Chemicals, Peptides, and Recombinant Proteins | | |
| Tamoxifen | Sigma-Aldrich | Cat# T5648-5G |
| Corn oil | Sigma-Aldrich | Cat# C8267-500ML |
| BrdU | Sigma-Aldrich | Cat# 19-160 |
| Recombinant IL-2 | Deprotech | Cat# 212-12 |
| Recombinant IL-7 | Deprotech | Cat# 217-17 |

| REAGENT or RESOURCE | SOURCE | IDENTIFIER |
|---|---|---|
| Recombinant IL-15 | Peprotech | Cat# 210-15 |
| Paraformaldehyde | Electron Microscopy Sciences | Cat# 50-980-487 |
| Myelin oligodendrocyte peptide | Anaspec | Cat# AS-60130-1 |
| Complete Freund's adjuvant | Difco | Cat# DF0638-60-7 |
| Pertussis toxin | List Biological | Cat# 181 |
| Methanol | Sigma-Aldrich | Cat# 322415-2L |
| Critical Commercial Assays | | |
| PrimeSTAR GXL DNA Polymerase | Takara | Cat# R050A |
| APC BrdU Flow Kit | Becton Dickinson | Cat# 552598 |
| APC Annexin-V Apoptosis Detection Kit | Becton Dickinson | Cat# 550474 |
| Seahorse XF Glycolysis Stress Test Kit | Seahorse Biosciences | Cat# 103020-100 |
| Experimental Models: Organisms/Strains | | |
| Mouse: CD25 fl/fl | This paper | N/A |
| Mouse: Rosa-Flpo: B6.129S4-*Gt(ROSA)26Sor*$^{tm2(FLP*)Sor}$/J | Jackson Laboratory | Cat# 012930 |
| Mouse: Rosa-RFP: Gt(ROSA)26Sor$^{tm1Hjf}$ | Luche et al., 2007 | MGI# 3696099 |
| Mouse: FoxP3-eGFP-Cre-ERT2: *Foxp3*$^{tm9(EGFP/cre/ERT2)Ayr}$/J | Jackson Laboratory | Cat# 016961 |
| Mouse: FoxP3-Cre-YFP: B6.129(Cg)-*Foxp3* $^{tm4(YFP/icre)Ayr}$/J | Jackson Laboratory | Cat# 016959 |
| Mouse: CD45.1+: B6.SJL-*Ptprc*$^{a}$ *Pepc*$^{b}$/BoyJ | Jackson Laboratory | Cat# 002014 |
| Mouse: IL-7 KO: Il7$^{tm1Dnax}$ | DNAX Research Institute | MGI# 1857652 |
| Mouse: IL-15 KO: C57BL/6NTac-*IL15*$^{tm1Imx}$ N5 | Taconic Biosciences | Cat# 4269 |
| Mouse: C57BL/6: C57BL/6 | Charles River | Cat# 027 |
| Software and Algorithms | | |
| Graph Pad Prism 7 | Graph Pad | N/A |
| FlowJo V10 | TreeStar | N/A |
| Other | | |
| RPMI-1640 | Lonza | Cat# 12-702Q |
| 2-Mercaptoethanol | Thermo Scientific | Cat# 31350010 |
| Penicillin/Streptomycin | Sigma-Aldrich | Cat# P4333-100ML |
| Fetal Bovine Serum | GIBCO | Cat# 10438026 |
| L-Glutamine | Sigma-Aldrich | Cat# G6392 |
| Histopaque 1119 | Sigma-Aldrich | Cat# 11191-100ML |
| Histopaque 1077 | Sigma-Aldrich | Cat# 10771-100ML |
| Collagenase II | Worthington | Cat# LS004176 |
| Phosphate-Buffered Saline pH 7.4 | GE Healthcare | Cat# SH30256.FS |
| 10× Hanks' Balanced Salt Solution | GIBCO | Cat# 14185052 |
| Mouse CD4+ T cell enrichment kit | Invitrogen | Cat# 8804-6821-74 |
| Intracellular Fixation & Permeabilization Buffer Set | eBioscience | Cat# 88-8824-00 |
| BD Phosflow Lyse/Fix Buffer | BD Biosciences | Cat# 558049 |
| BD Phosflow Perm Buffer III | BD Biosciences | Cat# 558050 |

## CONTACT FOR REAGENT AND RESOURCE SHARING

Further information and requests for resources and reagents should be directed to and will be fulfilled by the Lead Contact, Laurence A. Turka (lturka@partners.org).

## EXPERIMENTAL MODEL AND SUBJECT DETAILS

**Generation of CD25$^{fl/fl}$ mice—**Embryonic stem cells were obtained from the EUCOMM repository (Skarnes et al., 2011) and long range PCR (LRPCR; Takara Bio) was used to confirm homologous recombination at the *Il2ra* locus (Figures S1B and S1C), Chimeric mice were generated at the Brigham and Women's Transgenic core. A neomycin selection cassette in the targeted *Il2ra* allele was removed by breeding the F1 generation with a mouse line expressing Flp recombinase under control of the *Rosa* locus (Rosa-Flpo) (Raymond and Soriano, 2007) (Figures S1A, S1D, and S1E). The resulting allele was termed "CD25$^{fl}$" and used for all experiments. The Rosa-Flpo allele was deliberately removed while establishing mice homozygous for a RFP reporter at the *Rosa* locus.

**Animal Model Details—**CD45.1 $^{+}$ congenic, Rosa-Flpo, and Foxp3$^{eGFP\text{-}Cre\text{-}ERT2}$ mice were purchased from The Jackson Laboratory. Rosa-RFP reporter mice were a gift of H.J. Fehling and generously provided by S. Virgin. Foxp3$^{YFP\text{-}Cre}$ mice were a gift of A. Rudensky. These mice were maintained at Massachusetts General Hospital. IL-7$^{-/-}$, IL-15$^{-/-}$, and C57BL/6 (B6) mice were obtained by S.M. Kaech from Schering-Plough Biopharma, The Jackson Laboratory, and the National Cancer Institute respectively, and maintained at Yale University throughout the adoptive transfer experiments. Blood draws and adoptive cell transfers were performed through the retro-orbital route. Mice were housed in specific pathogen free conditions. Male and female mice, 6-8 weeks old, were used for all experiments. All experiments were approved by the Institutional Animal Care and Use Committees of Massachusetts General Hospital and Yale University.

## METHOD DETAILS

**Tamoxifen and BrdU administration—**Mice were given intraperitoneal injections of 1.5 mg tamoxifen in 100 uL corn oil (Sigma) each day for 4 consecutive days and sacrificed two weeks later, unless otherwise noted. For experiments involving BrdU, mice were additionally given intraperitoneal injections of 1 mg BrdU (Sigma) in 100 uL PBS(GE Healthcare) every 12 hr for 72 hr prior to sacrifice. BrdU incorporation was measured with the BrdU Flow Kit (BD) according to manufacturer's instructions.

**Tissue processing—**Secondary lymphoid organs (spleen, lymph nodes, or thymus) were homogenized through a 70 um filter using the back of a syringe plunger while being washed with FACS buffer (D-PBS $^{+}$ 2% FBS $^{+}$ 0.1% sodium azide $^{+}$ 2mM EDTA). Red blood cells (RBC) were removed by resuspension in Ack lysis buffer for 2 minutes, followed by washing in FACS buffer. Whole blood (250-300 uL) was processed by pipet mixing in 9 mL distilled water for 10 s, then immediately quenching with 1 mL 10x Hanks' Balanced Salt Solution. Cells were subsequently washed in FACS buffer. Visceral adipose tissue was cut into < 1mm fragments then digested with 1 mg/mL Collagenase II (Worthington) at 37°C for 20 minutes. Cells were then filtered through a 70 um filter. RBC were removed by resuspension in Ack lysis buffer for 30 s, followed by washing in FACS buffer. Liver was

first perfused by hepatic portal vein injection of Hanks' Balanced Salt Solution, then homogenized through a 70 um filter using the back of a syringe plunger while being washed with Hanks' Balanced Salt Solution. The homogenate was underlaid with a 22:50 mixture of Histopaque 1119:Histopaque 1077 (Sigma) and centrifuged at 2000 rpm for 20 minutes with no brake. The leukocyte layer was then collected and washed with FACS buffer.

**Flow cytometry—**Unless otherwise noted, staining for cell surface markers was performed in FACS buffer (D-PBS $^{+}$ 2% FBS $^{+}$ 0.1% sodium azide $^{+}$ 2mM EDTA) for 30 minutes at 4°C, using the antibodies described in Key Resources Table. For intracellular staining, fixation and permeabilization were performed according to manufacturer's recommendations. Annexin-Vx 7-AAD staining was performed using the APC Annexin-V Apoptosis Detection Kit (BD). Data were collected on LSR II or LSR Fortessa instruments (BD) and analyzed using FlowJo (BD). Cell sorting was performed using a FACS Aria instrument (BD).

***In vitro* suppression assay—**Two weeks after tamoxifen exposure, mice were sacrificed, and $CD4^{+}$ $RFP^{+}$ $Foxp3^{+}$ Tregs and $CD4^{+}$ $RFP^{-}$ $Foxp3^{-}$ Tconv were isolated by cell sorting. $RFP^{+}$ $Foxp3^{+}$ Tregs were stimulated overnight at 37*C with 5 ug/mL anti-CD3/CD28 (BioLegend) while $CD4^{+}$ $Foxp3^{-}$ Tconv were held at 4*C. Tregs were then co-cultured in 96-well U-bottom plates with 2*10^5 $CD4^{+}$ Tconv, anti-CD3/CD28 coated beads (Thermo), and APC conjugated anti-CD154 (MR1; BioLegend). After 7 hours cells were stained, fixed with the eBioscience Fixation/Permeabilization kit, and analyzed by flow cytometry.

***In vivo* suppression assay—**EAE was induced by subcutaneous immunization with 100 ug myelin oligodendrocyte peptide ($MOG_{35-55}$; Anaspec) in complete Freund's adjuvant, with 200 ng intraperitoneal pertussis toxin (List Biological) given on days 0 and 2 after immunization. To ensure the majority of Tregs were CD25-deleted throughout the course of the experiment, mice were given daily intraperitoneal injections of 1.5 mg tamoxifen in 100 uL corn oil (Sigma) on days 0-3 and 14-17 after immunization for a total of 8 tamoxifen injections. Disease progress and severity were assessed as published (Kohm et al., 2002). Briefly, mice were evaluated each day for disease score with a score of 0 = no paralysis, 1 = flaccid tail paralysis, 2 = partial hind limb paresis, 3 = bilateral hind limb paresis/paralysis, 4 = bilateral hind limb paralysis and partial forelimb paralysis, and 5 = moribund.

**Metabolism assay—**Extracellular acidification rate (ECAR) was measured by the glycolysis stress test of a XFe96 extracellular flux analyzer (Seahorse Bioscience). Two weeks after tamoxifen exposure, mice were sacrificed and $CD4^{+}$ $RFP^{+}$ $Foxp3^{+}$ Tregs were isolated by cell sorting. Cells were stimulated overnight with plate-bound anti-CD3 and anti-CD28 in the presence of 10 ng/mL IL-2, IL-7, or no cytokine. Tregs were then seeded into 96-well XF plates at 200,000 cells/well in glucose-free XF Assay media. ECAR measurements were taken according to manufacturer's instructions, first under resting conditions and then after the sequential addition of glucose (20 mM), oligomycin (1 μM), and 2-deoxy glucose (20 mM).

**Cytokine stimulation—**Two weeks after tamoxifen exposure, mice were sacrificed and $CD4^+$ $RFP^+$ $Foxp3^+$ Tregs were isolated by cell sorting. $RFP^+$ $Foxp3^+$ Tregs were stimulated overnight with 5 ug/mL plate-bound anti-CD3/CD28 (BioLegend). Cells were then washed, held at 37*C for 1 hr, and transferred to new wells lacking TCR stimulation. Cells were then incubated at 37*C for 24 hr with no cytokine or 10 ng/mL IL-2, IL-7, IL-15 (Peprotech). Surface staining was performed 15 minutes prior to harvest, at which point cells were immediately fixed with paraformaldehyde (Electron Microscopy Sciences) then permeabilized with methanol (Sigma). Cells were incubated with phospho-specific antibodies overnight, then analyzed by flow cytometry.

To evaluate STAT5 phosphorylation in unstimulated cells, bulk splenocytes rather than sorted cells were held 1 hr in 37*C serum-free RPMI, then exposed to cytokines for 20 minutes. Staining, fixation, and permeabilization was performed as described above.

**Primers—**A list of all primers can be found in Table S1.

### QUANTIFICATION AND STATISTICAL ANALYSIS

All statistical analysis was performed with Prism 7 (Graphpad). Statistical details, including statistical tests used, number of mice analyzed (n) can be found in the legend for each figure. Significance was defined as $p \leq 0.05$, with further stratification of p values reported as: not significant (ns) = $p > 0.05$, * = $p \leq 0.05$, ** = $p \leq 0.01$, *** = $p \leq 0.001$, **** = $p \leq 0.0001$. All error bars are represented as mean ± SD.

## Supplementary Material

Refer to Web version on PubMed Central for supplementary material.

## ACKNOWLEDGMENTS

We are grateful to the Brigham and Women's Transgenic core for their assistance in generating chimeric mice containing the CD25-fl allele. We thank A. Rudensky (Memorial Sloan Kettering Cancer Center) for $Foxp3^{YFP\text{-}Cre}$ mice and H.J. Fehling (Universität Ulm) for Rosa-RFP reporter mice. We are grateful to D. Kreamalmayer of the S. Virgin lab (Washington University in St. Louis) for his assistance in obtaining Rosa-RFP reporter mice. We thank S. Sakaguchi and N. Ohkura (Osaka University) for valuable discussions and feedback; A. Kohlgruber, V. Mani, and J. Kuchroo for technical assistance; and R. Newton, R. Zhang, J. Chang, D. Gadi, and members of the Turka lab for valuable discussions and technical assistance. The authors acknowledge financial support from the NIH (grant P01-HL018646 to L.A.T. and grant T32-AI007529 to M.Y.F.) and the Herchel Smith Graduate Fellowship Program (M.Y.F.).

## REFERENCES

Bielekova B, Catalfamo M, Reichert-Scrivner S, Packer A, Cerna M, Waldmann TA, McFarland H, Henkart PA, and Martin R (2006). Regulatory CD56(bright) natural killer cells mediate immunomodulatory effects of IL-2Ralpha-targeted therapy (daclizumab) in multiple sclerosis. Proc. Natl. Acad. Sci.USA 103, 5941–5946. [PubMed: 16585503]

Burchill MA, Yang J, Vogtenhuber C, Blazar BR, and Farrar MA (2007). IL-2 receptor beta-dependent STAT5 activation is required for the development of Foxp3+ regulatory T cells. J. Immunol. 178, 280–290. [PubMed: 17182565]

Canavan JB, Afzali B, Scottà C, Fazekasova H, Edozie FC, Macdonald TT, Hernandez-Fuentes MP, Lombardi G, and Lord GM (2012). A rapid diagnostic test for human regulatory T-cell function to enable regulatory T-cell therapy. Blood 119, e57–e66. [PubMed: 22219224]

Chinen T, Kannan AK, Levine AG, Fan X, Klein U, Zheng Y, Gasteiger G, Feng Y, Fontenot JD, and Rudensky AY (2016). An essential role for the IL-2 receptor in Treg cell function. Nat. Immunol. 17, 1322–1333. [PubMed: 27595233]

Cornish GH, Sinclair LV, and Cantrell DA (2006). Differential regulation of T-cell growth by IL-2 and IL-15. Blood 108, 600–608. [PubMed: 16569767]

Couper KN, Blount DG, de Souza JB, Suffia I, Belkaid Y, and Riley EM (2007). Incomplete depletion and rapid regeneration of Foxp3+ regulatory T cells following anti-CD25 treatment in malaria-infected mice. J. Immunol. 178, 4136–4146. [PubMed: 17371969]

Cui G, Hara T, Simmons S,Wagatsuma K, Abe A, Miyachi H, Kitano S, Ishii M, Tani-ichi S, and Ikuta K (2014). Characterization of the IL-15 niche in primary and secondary lymphoid organs in vivo. Proc. Natl. Acad. Sci. USA 111, 1915–1920. [PubMed: 24449915]

Cui G, Staron MM, Gray SM, Ho PC, Amezquita RA, Wu J, and Kaech SM (2015). IL-7-induced glycerol transport and TAG synthesis promotes memory CD8+ T cell longevity. Cell 161, 750–761. [PubMed: 25957683]

D'Cruz LM, and Klein L (2005). Development and function of agonist-induced CD25+Foxp3+ regulatory T cells in the absence of interleukin 2 signaling. Nat. Immunol. 6, 1152–1159. [PubMed: 16227983]

Fan MY, and Turka LA (2018). Immunometabolism and PI(3)K signaling as a link between IL-2, Foxp3 expression, and suppressor function in regulatory T cells. Front. Immunol. 9, 69. [PubMed: 29434595]

Fisson S, Darrasse-Jèze G, Litvinova E, Septier F, Klatzmann D, Liblau R, and Salomon BL (2003). Continuous activation of autoreactive CD4+ CD25+ regulatory T cells in the steady state. J. Exp. Med. 198, 737–746. [PubMed: 12939344]

Fontenot JD, Rasmussen JP, Gavin MA, and Rudensky AY (2005). A function for interleukin 2 in Foxp3-expressing regulatory T cells. Nat. Immunol. 6, 1142–1151. [PubMed: 16227984]

Gerriets VA, Kishton RJ, Johnson MO, Cohen S, Siska PJ, Nichols AG, Warmoes MO, de Cubas AA, MacIver NJ, Locasale JW, et al. (2016). Foxp3 and Toll-like receptor signaling balance $T_{reg}$ cell anabolic metabolism for suppression. Nat. Immunol. 17, 1459–1466. [PubMed: 27695003]

Hara T, Shitara S, Imai K, Miyachi H, Kitano S, Yao H, Tani-ichi S, and Ikuta K (2012). Identification of IL-7-producing cells in primary and secondary lymphoid organs using IL-7-GFP knock-in mice. J. Immunol. 189,1577–1584. [PubMed: 22786774]

Hori S, Nomura T, and Sakaguchi S (2003). Control of regulatory T cell development by the transcription factor Foxp3. Science 299, 1057–1061. [PubMed: 12522256]

Huynh A, DuPage M, Priyadharshini B, Sage PT, Quiros J, Borges CM, Townamchai N, Gerriets VA, Rathmell JC, Sharpe AH, et al. (2015). Control of PI(3) kinase in Treg cells maintains homeostasis and lineage stability. Nat. Immunol. 16, 188–196. [PubMed: 25559257]

Jagger A, Shimojima Y, Goronzy JJ, and Weyand CM (2014). Regulatory T cells and the immune aging process: a mini-review. Gerontology 60, 130–137. [PubMed: 24296590]

Kohm AP, Carpentier PA, Anger HA, and Miller SD (2002). Cutting edge: CD4+CD25+ regulatory T cells suppress antigen-specific autoreactive immune responses and central nervous system inflammation during active experimental autoimmune encephalomyelitis. J. Immunol. 169, 4712–4716. [PubMed: 12391178]

Kohm AP, McMahon JS, Podojil JR, Begolka WS, DeGutes M, Kasprowicz DJ, Ziegler SF, and Miller SD (2006). Cutting Edge: Anti-CD25 monoclonal antibody injection results in the functional inactivation, not depletion, of CD4+CD25+ T regulatory cells. J. Immunol. 176, 3301–3305. [PubMed: 16517695]

Leonard WJ, Depper JM, Crabtree GR, Rudikoff S, Pumphrey J, Robb RJ, Kronke M, Svetlik PB, Peffer NJ, Waldmann TA, et al. (1984). Molecular cloning and expression of cDNAs for the human interleukin-2 receptor. Nature 311, 626–631. [PubMed: 6090948]

Lio CW, and Hsieh CS (2008). A two-step process for thymic regulatory T cell development. Immunity 28, 100–111. [PubMed: 18199417]

Liu Z, Gerner MY, Van Panhuys N, Levine AG, Rudensky AY, and Germain RN (2015). Immune homeostasis enforced by co-localized effector and regulatory T cells. Nature 528, 225–230. [PubMed: 26605524]

Luche H, Weber O, Nageswara Rao T, Blum C, and Fehling HJ (2007). Faithful activation of an extra-bright red fluorescent protein in "knock-in" Crereporter mice ideally suited for lineage tracing studies. Eur. J. Immunol. 37, 43–53. [PubMed: 17171761]

Lynch L, Michelet X, Zhang S, Brennan PJ, Moseman A, Lester C, Besra G, Vomhof-Dekrey EE,Tighe M, Koay HF, et al. (2015). Regulatory iNKT cells lack expression of the transcription factor PLZF and control the homeostasis of T(reg) cells and macrophages in adipose tissue. Nat. Immunol. 16, 85–95. [PubMed: 25436972]

Malek TR (2008). The biology of interleukin-2. Annu. Rev. Immunol. 26, 453–479. [PubMed: 18062768]

Newton R, Priyadharshini B, and Turka LA (2016). Immunometabolism of regulatory T cells. Nat. Immunol. 17, 618–625. [PubMed: 27196520]

Nishioka T, Shimizu J, Iida R, Yamazaki S, and Sakaguchi S (2006). CD4+CD25+Foxp3+ T cells and CD4+CD25-Foxp3+ T cells in aged mice. J. Immunol. 176, 6586–6593. [PubMed: 16709816]

Onizuka S, Tawara I, Shimizu J, Sakaguchi S, Fujita T, and Nakayama E (1999). Tumor rejection by in vivo administration of anti-CD25 (interleukin-2 receptor alpha) monoclonal antibody. Cancer Res. 59, 3128–3133. [PubMed: 10397255]

Raymond CS, and Soriano P (2007). High-efficiency FLP and PhiC31 site-specific recombination in mammalian cells. PLoS ONE 2, e162. [PubMed: 17225864]

Raynor J, Sholl A, Plas DR, Bouillet P, Chougnet CA, and Hildeman DA (2013). IL-15 fosters age-driven regulatory T cell accrual in the face of declining IL-2 levels. Front. Immunol. 4, 161. [PubMed: 23805138]

Rech AJ, Mick R, Martin S, Recio A,Aqui NA, Powell DJ, Jr., Colligon TA, Trosko JA, Leinbach LI, Pletcher CH, et al. (2012). CD25 blockade depletes and selectively reprograms regulatory T cells in concert with immunotherapy in cancer patients. Sci. Transl. Med. 4, 134ra62.

Reichert JM, Rosensweig CJ, Faden LB, and Dewitz MC (2005). Monoclonal antibody successes in the clinic. Nat. Biotechnol. 23, 1073–1078. [PubMed: 16151394]

Ring AM, Lin JX, Feng D, Mitra S, Rickert M, Bowman GR, Pande VS, Li P, Moraga I, Spolski R, et al. (2012). Mechanistic and structural insight into the functional dichotomy between IL-2 and IL-15. Nat. Immunol. 13, 1187–1195. [PubMed: 23104097]

Rubtsov YP, Rasmussen JP, Chi EY, Fontenot J, Castelli L, Ye X, Treuting P, Siewe L, Roers A, Henderson WR, Jr., et al. (2008). Regulatory T cell-derived interleukin-10 limits inflammation at environmental interfaces. Immunity 28, 546–558. [PubMed: 18387831]

Rubtsov YP, Niec RE, Josefowicz S, Li L, Darce J, Mathis D, Benoist C, and Rudensky AY (2010). Stability of the regulatory T cell lineage in vivo. Science 329, 1667–1671. [PubMed: 20929851]

Ruitenberg JJ, Boyce C, Hingorani R, Putnam A, and Ghanekar SA (2011). Rapid assessment of in vitro expanded human regulatory T cell function. J. Immunol. Methods 372, 95–106. [PubMed: 21781972]

Sadlack B, Merz H, Schorle H, Schimpl A, Feller AC, and Horak I (1993). Ulcerative colitis-like disease in mice with a disrupted interleukin-2 gene. Cell 75, 253–261. [PubMed: 8402910]

Sakaguchi S, Sakaguchi N, Asano M, Itoh M, and Toda M (1995). Immunologic self-tolerance maintained by activated T cells expressing IL-2 receptor alpha-chains (CD25). Breakdown of a single mechanism of self-tolerance causes various autoimmune diseases. J. Immunol. 155, 1151–1164. [PubMed: 7636184]

Setiady YY, Coccia JA, and Park PU (2010). In vivo depletion of CD4+FOXP3+Treg cells by the PC61 anti-CD25 monoclonal antibody is mediated by FcgammaRIII+ phagocytes. Eur. J. Immunol. 40, 780–786. [PubMed: 20039297]

Setoguchi R, Hori S, Takahashi T, and Sakaguchi S (2005). Homeostatic maintenance of natural Foxp3(+) CD25(+) CD4(+) regulatory T cells by interleukin (IL)-2 and induction of autoimmune disease by IL-2 neutralization. J. Exp. Med. 201, 723–735. [PubMed: 15753206]

Sharfe N, Dadi HK, Shahar M, and Roifman CM (1997). Human immune disorder arising from mutation of the alpha chain of the interleukin-2 receptor. Proc. Natl. Acad. Sci. USA 94, 3168–3171. [PubMed: 9096364]

Skarnes WC, Rosen B, West AP, Koutsourakis M, Bushell W, Iyer V, Mujica AO, Thomas M, Harrow J, Cox T, et al. (2011). A conditional knockout resource for the genome-wide study of mouse gene function. Nature 474, 337–342. [PubMed: 21677750]

Smigiel KS, Richards E, Srivastava S, Thomas KR, Dudda JC, Klonowski KD, and Campbell DJ (2014). CCR7 provides localized access to IL-2 and defines homeostatically distinct regulatory T cell subsets. J. Exp. Med. 211, 121–136. [PubMed: 24378538]

Stauber DJ, Debler EW, Horton PA, Smith KA, and Wilson IA (2006). Crystal structure of the IL-2 signaling complex: paradigm for a heterotrimeric cytokine receptor. Proc. Natl. Acad. Sci. USA 103, 2788–2793. [PubMed: 16477002]

Vahl JC, Drees C, Heger K, Heink S, Fischer JC, Nedjic J, Ohkura N, Morikawa H, Poeck H, Schallenberg S, et al. (2014). Continuous T cell receptor signals maintain a functional regulatory T cell pool. Immunity 41, 722–736. [PubMed: 25464853]

Vang KB, Yang J, Mahmud SA, Burchill MA, Vegoe AL, and Farrar MA (2008). IL-2, −7, and −15, but not thymic stromal lymphopoeitin, redundantly govern CD4+Foxp3+ regulatory T cell development. J. Immunol. 181, 3285–3290. [PubMed: 18714000]

Willerford DM, Chen J, Ferry JA, Davidson L, Ma A, and Alt FW (1995). Interleukin-2 receptor alpha chain regulates the size and content of the peripheral lymphoid compartment. Immunity 3, 521–530. [PubMed: 7584142]

Zeng H, Yang K, Cloer C, Neale G, Vogel P, and Chi H (2013). mTORC1 couples immune signals and metabolic programming to establish T(reg)-cell function. Nature 499, 485–490. [PubMed: 23812589]

Zorn E, Nelson EA, Mohseni M, Porcheray F, Kim H, Litsa D, Bellucci R, Raderschall E, Canning C, Soiffer RJ, et al. (2006). IL-2 regulates FOXP3 expression in human CD4+CD25+ regulatory T cells through a STAT-dependent mechanism and induces the expansion of these cells in vivo. Blood 108, 1571–1579. [PubMed: 16645171]

## Highlights

- IL-2 signaling is needed for the long-term survival of most major Treg subsets
- In the absence of IL-2 signaling, Tregs may temporarily persist on IL-7 *in vivo*
- Treg glycolysis and suppressor function are reduced in the absence of IL-2
- IL-2 signaling is not necessary to maintain Treg lineage stability *in vivo*

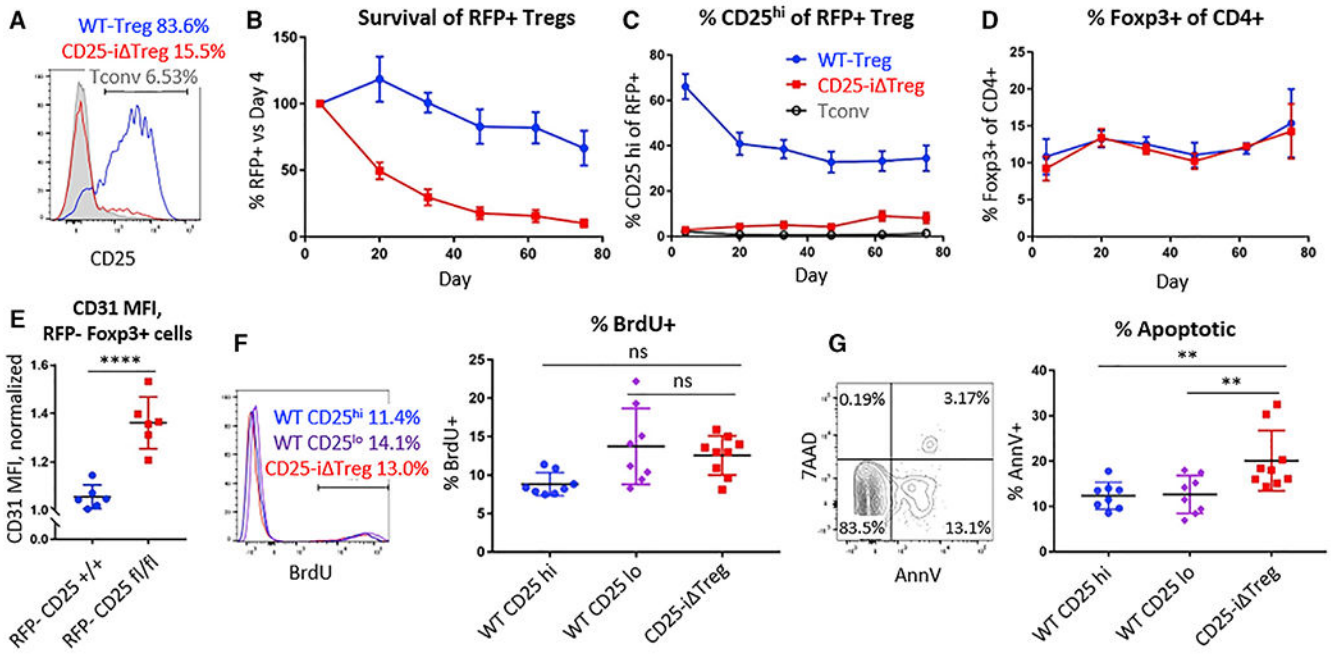


**Figure 1. Loss of Tregs following CD25 Deletion**

(A) Sample CD25 gating for $CD4^+$ $Foxp3^+$ $RFP^+$ Tregs showing cutoffs for $CD25^{hi}$ cells. WT-Tregs may be stratified into WT $CD25^{hi}$ and WT $CD25^{lo}$ subsets, while CD25-iΔTregs are defined as $CD25^-$ cells.

(B) Prevalence of $RFP^+$ $Foxp3^+$ cells in blood over time, normalized to initial levels measured 4 days after the first tamoxifen injection.

(C and D) Proportion of $CD25^{hi}$ cells among $RFP^+$ $Foxp3^+$ cells (C) and proportion of $Foxp3^+$ cells among $CD4^+$ T cells (D) over time.

(E) Expression of CD31, a marker of recent thymic emigrants, among $RFP^-$ $CD25^{fl/fl}$ and $RFP^-$ $CD25^{+/+}$ Tregs 2 weeks after tamoxifen injection.

(F and G) BrdU uptake (F) and Annexin-V binding (G) among WT $CD25^{hi}$, WT $CD25^{lo}$ and CD25-iΔTregs 2 weeks following tamoxifen injection. Representative gating is shown to the left of each graph.

MFI, mean fluorescent intensity. Values shown are mean ± SD. Data were analyzed using a two-tailed Student's t test, n = 6 mice (E), or a one-way ANOVA with Tukey's post-test correction, n = 8–9 mice (F and G). $^{**}p < 0.01$, $^{****}p < 0.0001$. See also Figure S4.

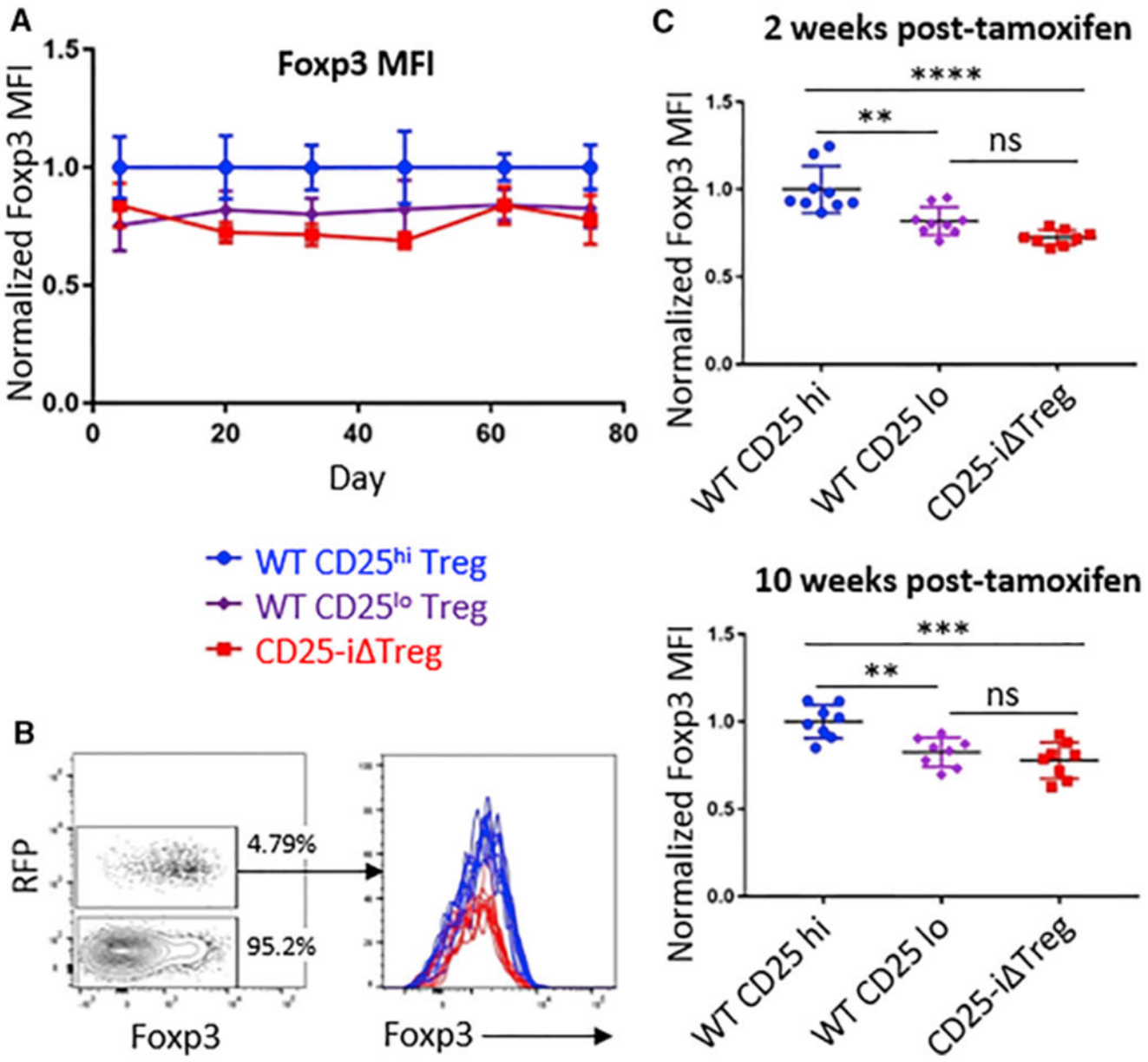


**Figure 2. CD25-iΔTregs Have Reduced Foxp3 Expression but Maintain Lineage Stability**

(A) Foxp3 levels among WT CD25$^{hi}$, WT CD25$^{lo}$, and CD25-iΔTregs following tamoxifen injection.

(B) Left: representative gating of RFP$^{+}$ cells to measure Foxp3 expression. Right: Foxp3 histograms, with each line representing a histogram from an individual mouse 10 weeks after tamoxifen administration.

(C) Foxp3 expression among WT CD25$^{hi}$, WT CD25$^{lo}$, and CD25-iΔTregs at 2 weeks (left) and 10 weeks (right) after tamoxifen administration.

MFI, mean fluorescent intensity. Values shown are mean ± SD. Data were analyzed using a one-way ANOVA with Tukey's post-test correction. n = 8–9 mice, **p < 0.01, ***p < 0.001, ****p < 0.0001.

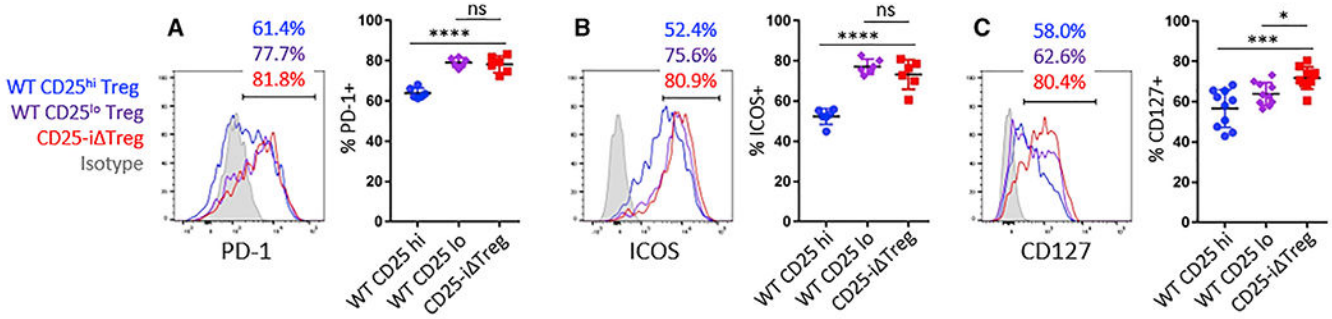


**Figure 3. Surface Staining of CD25-iΔTregs Resembles that of WT CD25$^{lo}$ Tregs**

Splenic RFP$^{+}$ Foxp3$^{+}$ Tregs were analyzed by flow cytometry 2 weeks after tamoxifen injection for expression of major Treg surface proteins, including PD-1 (A) and ICOS (B) and CD127, the IL-7 receptor alpha subunit (C). For each marker, representative histograms are shown at top. MFI, mean fluorescent intensity.

Values shown are mean ± SD. Data were analyzed using a one-way ANOVA with Tukey's post-test correction, n = 6–8 mice. *p < 0.05, ***p < 0.001, ****p < 0.0001.

See also Figure S5.

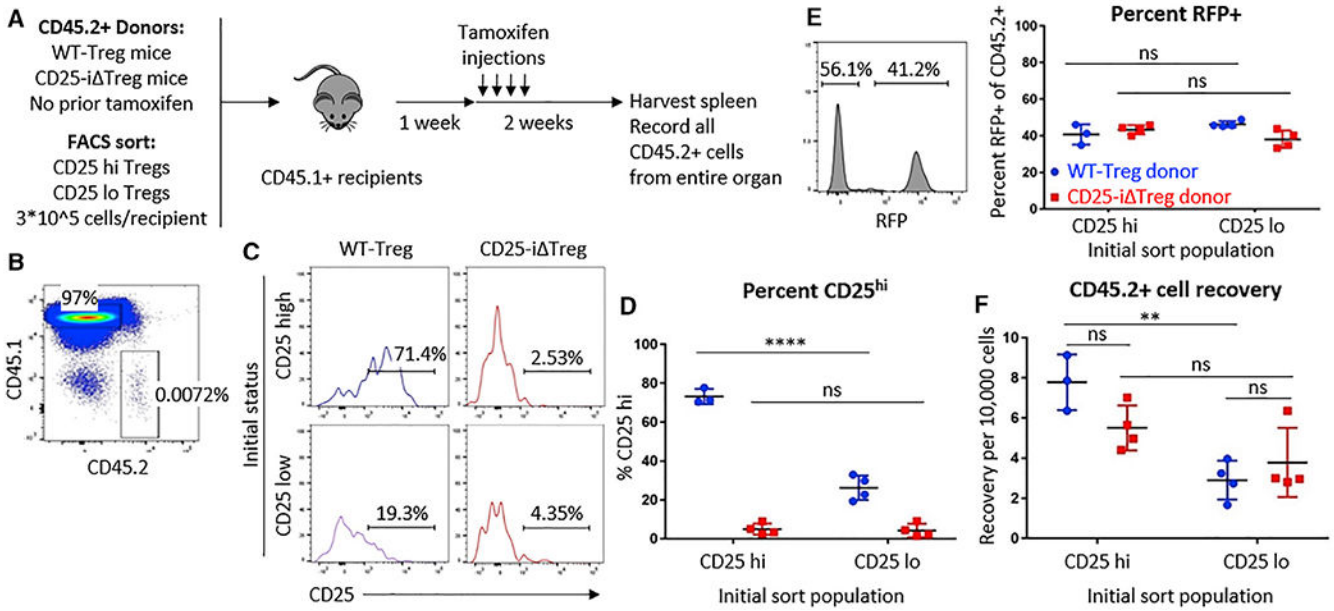


**Figure 4. Survival of CD25$^{hi}$ Tregs following CD25 Deletion**

(A) Tamoxifen-untreated CD25$^{hi}$ or CD25$^{lo}$ Tregs were sorted from WT-Treg or CD25-iΔTreg donors and transferred into separate CD45.1 $^{+}$ recipients. Mice were allowed 1 week to rest, injected with tamoxifen, and sacrificed 2 weeks later.

(B) Sample plot showing recovery of donor CD45.2$^{+}$ cells.

(C) Sample CD25 histograms of recovered CD45.2$^{+}$ Tregs, showing cutoffs for CD25$^{hi}$ cells.

(D) Quantification of CD25$^{hi}$ cells among recovered Tregs.

(E) Percentage of RFP$^{+}$ cells among CD45.2$^{+}$ cells. Representative histogram of RFP expression shown left.

(F) Recovery of donor cells following tamoxifen treatment.

Values shown are mean ± SD. Data were analyzed using a two-way ANOVA with Tukey's post-test correction, n = 3–4 mice. **p < 0.01, ****p < 0.0001.

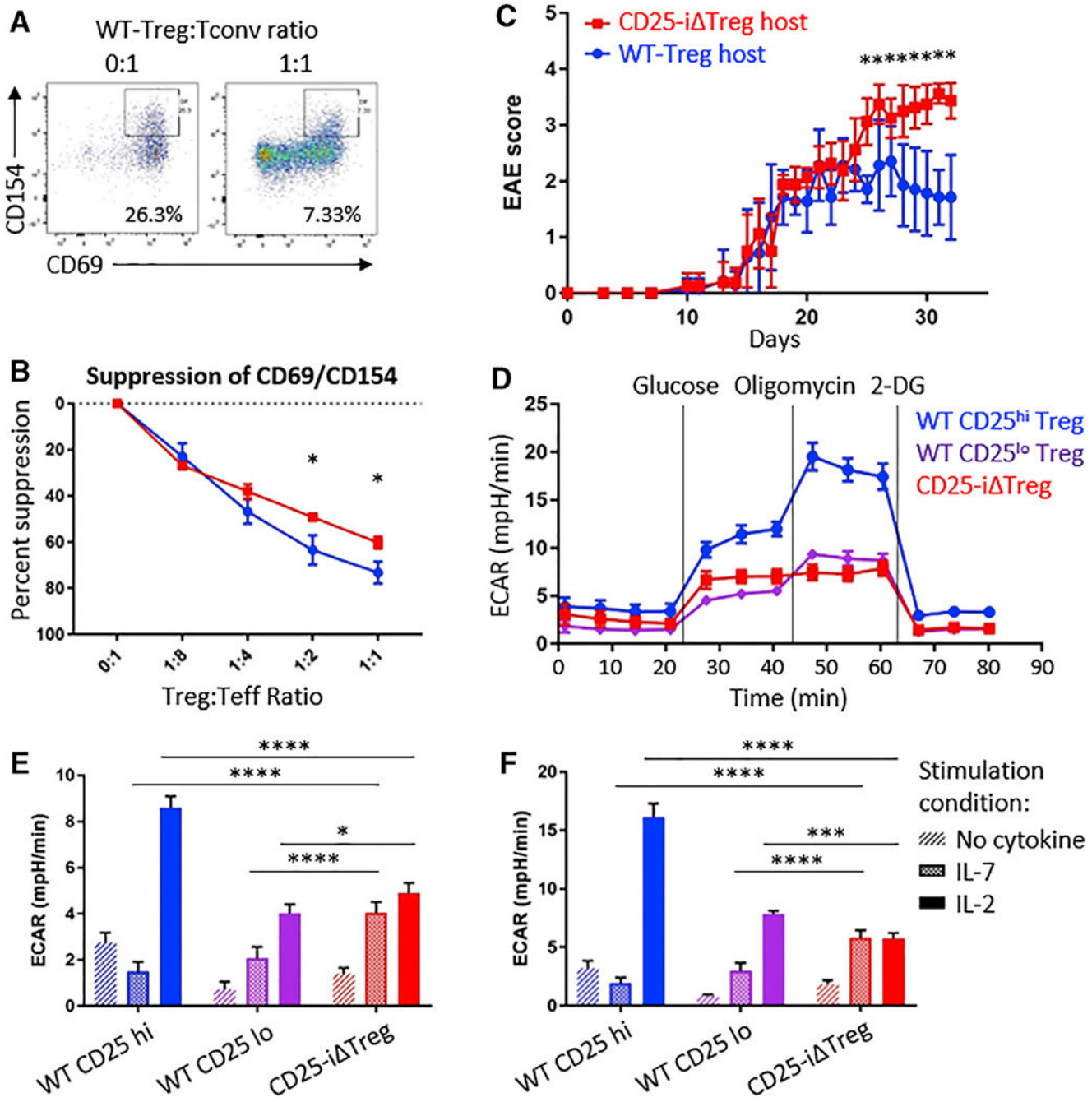


**Figure 5. Reduced Suppressor Function and Glycolysis among CD25-iΔTregs**

(A) Sample gating showing dual expression of CD69 and CD154 among $1 \times 10^5$ target Foxp3$^-$ CD4$^+$ T cells in the absence (left) or presence (right) of an equal number of WT-Tregs.

(B) Rapid *in vitro* suppression assay of target cells by titrated numbers of CD25-iΔTregs and WT-Tregs.

(C) Clinical severity of EAE in WT-Treg and CD25-iΔTreg mice. Mice were immunized with myelin oligodendrocyte peptide and monitored for 1 month. Tamoxifen was administered at the same time as EAE induction and again 2 weeks later.
(D) Representative glycolysis stress test of WT $CD25^{hi}$, WT $CD25^{lo}$, and CD25-iΔTregs following overnight stimulation in the presence of IL-2. A Seahorse flux analyzer was used to measure extracellular acidification rate (ECAR) of Tregs at baseline and then after treatment with glucose, oligomycin, and 2-deoxyglucose (2-DG) (treatment time, vertical dotted lines).
(E and F) Treg glycolytic rate (E) and glycolytic capacity (F) following overnight stimulation in the presence of no cytokine, IL-2, or IL-7.
Values shown are mean ± SD. Data were analyzed using a two-tailed Student's t test, n = 4–5 mice (B) or n = 8–9 mice (C), or a two-way ANOVA with Tukey's post-test correction, n = 5–6 mice (E and F). *p < 0.05, ***p < 0.001, ****p < 0.0001.

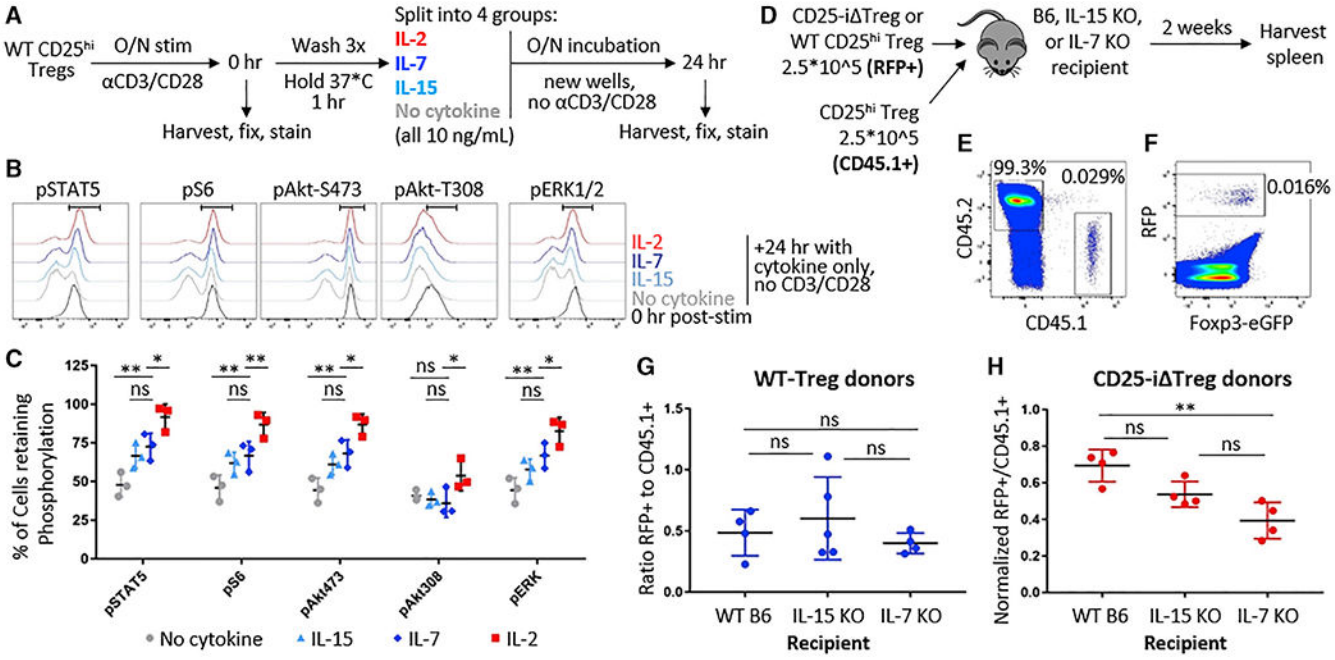


**Figure 6. Concomitant Deprivation of IL-7, but Not IL-15, Exacerbates Treg Loss following CD25 Deletion**

(A) Schematic for evaluating efficacy of IL-2, IL-7, and IL-15 at maintaining downstream signals. WT CD25$^{hi}$ Tregs were stimulated overnight, removed from stimulation, and then incubated with one of three cytokines for another 24 hr.

(B and C) Maintenance of downstream phosphorylation by IL-2, IL-7, and IL-15. Bars in representative histograms (B) indicate cutoffs for cells retaining phosphorylation.

(D) CD25-iΔTregs or WT CD25$^{hi}$ Tregs were adoptively transferred into IL-15 KO or IL-7 KO recipients, with an equal number of CD45.1$^{+}$ CD25$^{hi}$ cells. Recipient mice were sacrificed after 2 weeks.

(E and F) Sample gates are shown for recovery of CD45.1$^{+}$ cells (E) and RFP$^{+}$ Tregs (F).

(G and H) Recovery of WT-Tregs (G) and CD25-iΔTregs (H) following 2 weeks of IL-15 or IL-7 deprivation *in vivo.*

Values shown are mean ± SD. Data were analyzed using a one-way ANOVA with Dunnett's post-test correction, n = 3 samples (C), or a one-way ANOVA with Tukey's post-test correction, n = 4–5 mice (G and H). *p < 0.05, **p < 0.01. See also Figure S6.

| REAGENT or RESOURCE | SOURCE | IDENTIFIER |
|---|---|---|
| Antibodies | | |
| anti-CD25, clone PC61 | BioLegend | Cat# 102033; RRID:A3_10895908 |
| anti-CD4, clone GK1.5 | BioLegend | Cat# 100434; RRID:A3_893324 |
| anti-CD8, clone 53-6.7 | BioLegend | Cat# 100734; RRID:A3_2075238 |
| anti-CD45.2, clone 104 | BioLegend | Cat# 109824; RRID:A3_830789 |
| anti-CD45.1, clone A20 | BioLegend | Cat# 110716; RRID:A3_313505 |
| anti-CD62L, clone MEL-14 | BioLegend | Cat# 104411; RRID:A3_313098 |
| anti-CD44, clone IM7 | BioLegend | Cat# 103023; RRID:A3_493686 |
| anti-CD69, clone H1.2F3 | BioLegend | Cat# 104527; RRID:A3_10900250 |
| anti-CD31, clone 390 | BioLegend | Cat# 102415; RRID:A3_493411 |
| anti-CD127, clone A7R34 | BioLegend | Cat# 135023; RRID:A3_10897948 |
| anti-CD122, clone TM-β1 | BioLegend | Cat# 123209; RRID:A3_940615 |
| anti-CD132, clone TUGm2 | BioLegend | Cat# 132307; RRID:A3_10643575 |
| anti-PD-1, clone RMP1-30 | BioLegend | Cat# 109109; RRID:A3_572016 |
| anti-ICOS, clone 7E.17G9 | BioLegend | Cat# 117406; RRID:A3_2122712 |
| anti-GITR, clone DTA-1 | BioLegend | Cat# 126311; RRID:A3_1134212 |
| anti-CTLA-4, clone UC10-4B9 | BioLegend | Cat# 106309; RRID:A3_2230158 |
| anti-Nrp-1, clone 3E12 | BioLegend | Cat# 145206; RRID:A3_2562032 |
| anti-CD25, clone 7D4 | eBioscience | Cat# 13-0252-82; RRID:A3_891428 |
| anti-CD215, clone DNT15Ra | eBioscience | Cat# 17-7149-82; RRID:A3_10718543 |
| anti-Helios, clone 22F6 | BioLegend | Cat# 137220; RRID:A3_10690535 |
| anti-Foxp3, clone FJK-16 s | eBioscience | Cat# 53-5773-82; RRID:A3_763537 |
| anti-p-STAT5, clone SRBCZX | eBioscience | Cat# 17-9010-41; RRID:A3_2573271 |
| anti-p-S6, clone cupk43k | eBioscience | Cat# 17-9007-42; RRID:A3_2573270 |
| anti-p-Akt, Ser473, clone SDRNR | eBioscience | Cat# 48-9715-41; RRID:A3_2574124 |
| anti-p-ERK1/2, clone MILAN8R | eBioscience | Cat# 17-9109-41; RRID:A3_2573293 |
| anti-p-Akt, Thr308, polyclonal | Cell Signaling Technology | Cat# 9275S; RRID:A3_329828 |
| anti-PTEN, clone A2B1 | BD Biosciences | Cat# 560003; RRID:A3_1645437 |
| anti-CD154, clone MR1 | BioLegend | Cat# 106510; RRID:A3_2561561 |
| LEAF purified anti-CD3, clone 2C11 | BioLegend | Cat# 100314; RRID:A3_312679 |
| LEAF purified anti-CD28, clone 37.51 | BioLegend | Cat# 102112; RRID:A3_312877 |
| Dynabeads Mouse T-Activator CD3/CD28 | Thermo Scientific | Cat# 11456D |
| Chemicals, Peptides, and Recombinant Proteins | | |
| Tamoxifen | Sigma-Aldrich | Cat# T5648-5G |
| Corn oil | Sigma-Aldrich | Cat# C8267-500ML |
| BrdU | Sigma-Aldrich | Cat# 19-160 |
| Recombinant IL-2 | Deprotech | Cat# 212-12 |
| Recombinant IL-7 | Deprotech | Cat# 217-17 |

| REAGENT or RESOURCE | SOURCE | IDENTIFIER |
|---|---|---|
| Recombinant IL-15 | Peprotech | Cat# 210-15 |
| Paraformaldehyde | Electron Microscopy Sciences | Cat# 50-980-487 |
| Myelin oligodendrocyte peptide | Anaspec | Cat# AS-60130-1 |
| Complete Freund's adjuvant | Difco | Cat# DF0638-60-7 |
| Pertussis toxin | List Biological | Cat# 181 |
| Methanol | Sigma-Aldrich | Cat# 322415-2L |
| Critical Commercial Assays | | |
| PrimeSTAR GXL DNA Polymerase | Takara | Cat# R050A |
| APC BrdU Flow Kit | Becton Dickinson | Cat# 552598 |
| APC Annexin-V Apoptosis Detection Kit | Becton Dickinson | Cat# 550474 |
| Seahorse XF Glycolysis Stress Test Kit | Seahorse Biosciences | Cat# 103020-100 |
| Experimental Models: Organisms/Strains | | |
| Mouse: CD25 fl/fl | This paper | N/A |
| Mouse: Rosa-Flpo: B6.129S4-*Gt(ROSA)26Sor*$^{tm2(FLP*)Sor}$/J | Jackson Laboratory | Cat# 012930 |
| Mouse: Rosa-RFP: Gt(ROSA)26Sor$^{tm1Hjf}$ | Luche et al., 2007 | MGI# 3696099 |
| Mouse: FoxP3-eGFP-Cre-ERT2: *Foxp3*$^{tm9(EGFP/cre/ERT2)Ayr}$/J | Jackson Laboratory | Cat# 016961 |
| Mouse: FoxP3-Cre-YFP: B6.129(Cg)-*Foxp3* $^{tm4(YFP/icre)Ayr}$/J | Jackson Laboratory | Cat# 016959 |
| Mouse: CD45.1+: B6.SJL-*Ptprc*$^{a}$ *Pepc*$^{b}$/BoyJ | Jackson Laboratory | Cat# 002014 |
| Mouse: IL-7 KO: Il7$^{tm1Dnax}$ | DNAX Research Institute | MGI# 1857652 |
| Mouse: IL-15 KO: C57BL/6NTac-*IL15*$^{tm1Imx}$ N5 | Taconic Biosciences | Cat# 4269 |
| Mouse: C57BL/6: C57BL/6 | Charles River | Cat# 027 |
| Software and Algorithms | | |
| Graph Pad Prism 7 | Graph Pad | N/A |
| FlowJo V10 | TreeStar | N/A |
| Other | | |
| RPMI-1640 | Lonza | Cat# 12-702Q |
| 2-Mercaptoethanol | Thermo Scientific | Cat# 31350010 |
| Penicillin/Streptomycin | Sigma-Aldrich | Cat# P4333-100ML |
| Fetal Bovine Serum | GIBCO | Cat# 10438026 |
| L-Glutamine | Sigma-Aldrich | Cat# G6392 |
| Histopaque 1119 | Sigma-Aldrich | Cat# 11191-100ML |
| Histopaque 1077 | Sigma-Aldrich | Cat# 10771-100ML |
| Collagenase II | Worthington | Cat# LS004176 |
| Phosphate-Buffered Saline pH 7.4 | GE Healthcare | Cat# SH30256.FS |
| 10× Hanks' Balanced Salt Solution | GIBCO | Cat# 14185052 |
| Mouse CD4+ T cell enrichment kit | Invitrogen | Cat# 8804-6821-74 |
| Intracellular Fixation & Permeabilization Buffer Set | eBioscience | Cat# 88-8824-00 |
| BD Phosflow Lyse/Fix Buffer | BD Biosciences | Cat# 558049 |
| BD Phosflow Perm Buffer III | BD Biosciences | Cat# 558050 |